UNIVERSITY OF AMSTERDAM

UvA-DARE (Digital Academic Repository)

Microglia Transcriptional Profiling in Major Depressive Disorder Shows Inhibition of Cortical Gray Matter Microglia

Scheepstra, K.W.F.; Mizee, M.R.; van Scheppingen, J.; Adelia, A.; Wever, D.D.; Mason, M.R.J.; Dubbelaar, M.L.; Hsiao, C.C.; Eggen, B.J.L.; Hamann, J.; Huitinga, I.

DOI
10.1016/j.biopsych.2023.04.020

Publication date
2023

Document Version
Final published version

Published in
Biological Psychiatry

License
CC BY

Link to publication

Citation for published version (APA):
Scheepstra, K. W. F., Mizee, M. R., van Scheppingen, J., Adelia, A., Wever, D. D., Mason, M. R. J., Dubbelaar, M. L., Hsiao, C. C., Eggen, B. J. L., Hamann, J., & Huitinga, I. (2023). Microglia Transcriptional Profiling in Major Depressive Disorder Shows Inhibition of Cortical Gray Matter Microglia. *Biological Psychiatry*, *94*(8), 619-629. https://doi.org/10.1016/j.biopsych.2023.04.020

General rights
It is not permitted to download or to forward/distribute the text or part of it without the consent of the author(s) and/or copyright holder(s), other than for strictly personal, individual use, unless the work is under an open content license (like Creative Commons).

Disclaimer/Complaints regulations
If you believe that digital publication of certain material infringes any of your rights or (privacy) interests, please let the Library know, stating your reasons. In case of a legitimate complaint, the Library will make the material inaccessible and/or remove it from the website. Please Ask the Library: https://uba.uva.nl/en/contact, or a letter to: Library of the University of Amsterdam, Secretariat, Singel 425, 1012 WP Amsterdam, The Netherlands. You will be contacted as soon as possible.

UvA-DARE is a service provided by the library of the University of Amsterdam (https://dare.uva.nl)

Download date:26 Mar 2025

Archival Report

Biological Psychiatry

Microglia Transcriptional Profiling in Major Depressive Disorder Shows Inhibition of Cortical Gray Matter Microglia

Karel W.F. Scheepstra, Mark R. Mizee, Jackelien van Scheppingen, Adelia Adelia, Dennis D. Wever, Matthew R.J. Mason, Marissa L. Dubbelaar, Cheng-Chih Hsiao, Bart J.L. Eggen, Jörg Hamann, and Inge Huitinga

ABSTRACT

BACKGROUND: Microglia have been implicated in the pathophysiology of major depressive disorder (MDD), but information on biological mechanisms is limited. Therefore, we investigated the gene expression profile of microglial cells in relation to neuronal regulators of microglia activity in well-characterized MDD and control autopsy brains.

METHODS: Pure, intact microglia were isolated at brain autopsy from occipital cortex gray matter (GM) and corpus callosum white matter of 13 donors with MDD and 10 age-matched control donors for RNA sequencing. Top differentially expressed genes were validated using immunohistochemistry staining. Because gene expression changes were only detected in GM microglia, neuronal regulators of microglia were investigated in cortical tissue and synaptosomes from the cortex by reverse transcriptase–quantitative polymerase chain reaction and Western blot.

RESULTS: Transcriptome analysis revealed 92 genes differentially expressed in microglia isolated from GM, but none in microglia from white matter in donors with MDD, compared with control donors. Of these, 81 genes were less abundantly expressed in GM in MDD, including *CD163*, *MKI67*, *SPP1*, *CD14*, *FCGR1A/C*, and *C1QA/B/C*. Accordingly, pathways related to effector mechanisms, such as the complement system and phagocytosis, were differentially regulated in GM microglia in MDD. Immunohistochemistry staining revealed significantly lower expression of CD163 protein in MDD. Whole tissue analysis showed an increase in *CD200* (p = .0009) and *CD47* (p = .068) messenger RNA, and CD47 protein was significantly elevated (p = .0396) in synaptic fractions of MDD cases.

CONCLUSIONS: Transcriptional profiling indicates an immune-suppressed microglial phenotype in MDD that is possibly caused by neuronal regulation.

https://doi.org/10.1016/j.biopsych.2023.04.020

Major depressive disorder (MDD) is a significant contributor to the global burden of disease and a leading cause of disability worldwide (1). Insight into disease pathophysiology and novel therapeutics are urgently needed because treatment resistance is common and occurs in up to 30% of patients with MDD (2). Among others, inflammation is a prominent hypothesis in the neurobiology of depression, based on altered levels of pro- and anti-inflammatory cytokines and chemokines in blood and postmortem brain tissue in MDD (3–5). Furthermore, a higher prevalence of MDD has been associated with chronic inflammatory diseases, such as rheumatoid arthritis, inflammatory bowel diseases, and multiple sclerosis (6,7). Peripheral and central inflammation alters microglia activity (8–10), which may alter neuronal functioning through mechanisms such as synapse stripping (11). Indeed, recent studies have shown an altered immune status of microglia in MDD (12,13).

Microglia account for 10% to 15% of the cells in the brain and influence major aspects of neuronal functioning. By surveilling the brain for debris, excessive proteins, dysfunctional synapses, and aberrant neurons, they regulate synaptic transmission and neural plasticity in health and disease (14). In psychiatric disorders, microglial changes have been demonstrated in schizophrenia, autism spectrum disorder, MDD, and bipolar disorder (13,15,16). However, it remains uncertain whether—and in which state—microglia have beneficial or detrimental effects in different neuropathological conditions. Studies of MDD have yielded contradicting results ranging from reactive microglia to microglia in a homeostatic state. Torres-Platas *et al.* (17) showed vascular infiltration of macrophages and reactive/primed microglia in the white matter (WM) of the dorsal anterior cingulate cortex of brains of donors with MDD who had committed suicide. In contrast, a positron emission tomography study with a radio-labeled tracer for translocator protein (TSPO)—a marker for microglial activation—showed no increase of reactive microglia and even lower TSPO levels in mild to moderate MDD (18). Another TSPO study showed increased binding in the dorsal anterior cingulate cortex exclusively in patients with moderate to

SEE COMMENTARY ON PAGE 602

© 2023 Society of Biological Psychiatry. This is an open access article under the CC BY license (http://creativecommons.org/licenses/by/4.0/).

ISSN: 0006-3223

Biological Psychiatry October 15, 2023; 94:619–629 www.sobp.org/journal

severe MDD with suicidal thoughts (19). Finally, two recent postmortem studies showed a noninflammatory signature of microglia, with upregulated homeostatic molecules (TMEM119, CX3CR1, and CD195) and downregulated immune activation markers (CD163, CD14, CD68, and HLA-DR) (12,13).

These contradictory findings regarding microglia in MDD prompted us to investigate their MDD-associated properties. Here, we investigated the transcriptome of primary human microglia in the tissue of a clinically well-characterized MDD brain donor cohort and gene and protein expression of neuronal regulators of microglia in an independent cohort.

METHODS AND MATERIALS

Human Postmortem Tissue

Human brain occipital cortex gray matter (GM) and corpus callosum WM was provided by the Netherlands Brain Bank (https://www.brainbank.nl). Informed consent to perform the autopsy and use tissue and clinical data for research purposes were obtained from all donors. All procedures were approved by the Medical Ethics Committee of Amsterdam University Medical Centers. For RNA sequencing, GM and WM tissue blocks were collected from the occipital cortex and corpus callosum of donors with MDD (n = 13) and age-matched non-neurological control donors (n = 10). Non-neurological control donors with cognitive problems, based on clinical data, were excluded from the analysis. Donor characteristics are summarized in Table 1 and displayed in detail in Table S1.

For immunohistochemistry and reverse transcriptase–quantitative polymerase chain reaction (RT-qPCR), independently collected GM tissue blocks from the occipital cortex of donors with MDD and age-matched non-neurological control donors were explored. Detailed donor characteristics are presented in Table S2.

Microglia Isolation

Corpus callosum and occipital cortex tissue blocks of 5 to 15 g were dissected at autopsy and stored in Hibernate A medium (Invitrogen) at 4 °C until further processing. Microglia isolations were performed as described before (20,21). Briefly, brain tissue was mechanically dissociated using a tissue homogenizer (VWR) followed by enzymatic digestion with trypsin for 45 minutes at 37 °C in Hibernate A medium supplemented with DNAse I (Roche). Percoll (GE Healthcare) density centrifugation was performed, and glial cells were collected from the interlayer. Magnetic-activated cell sorting was performed for positive selection of microglia using anti-CD11b beads (Miltenyi Biotec). Viable cells were counted, and the cell pellet was stored in 1 mL cold TRIsure (Bioline) at −80 °C for further analysis. To assess the purity of isolated cells, CD45, CD11b, and CD15 expression was analyzed by flow cytometry (Figure S1). Consistent with previous reports, WM and GM microglia expressed comparable levels of CD11b, while CD45 expression was higher in WM than in GM microglia (20,21).

Table 1. Characteristics of Donors With MDD and Control Donors Used for RNA Sequencing of Isolated Microglia

Donors	Sex, F/M, n	Age at Death, Years	PMD, Hours	pH CSF
Control, n = 10	5/5	75.0 ± 3.6	7.2 ± 0.5	6.8 ± 0.1
MDD, n = 13	7/6	63.7 ± 4.0	8.0 ± 0.7	6.7 ± 0.1

Data are presented as mean ± SEM.

CSF, cerebrospinal fluid; F, female; M, male; MDD, major depressive disorder; PMD, postmortem delay.

RNA Isolation

RNA isolation was carried out by QIAzol Lysis Reagent (Qiagen) according to the manufacturer's protocol using phase separation by chloroform addition and centrifugation followed by overnight precipitation in isopropanol at −20 °C. RNA concentration was measured using a NanoDrop (ND-1000; NanoDrop Technologies), and RNA integrity was assessed using a Bioanalyzer (2100; Agilent Technologies).

RNA Sequencing

RNA sequencing was performed by GenomeScan. Samples were prepared using the NEBNext Ultra Directional RNA Library Prep Kit from Illumina (NEB #E7420). Briefly, ribosomal RNA was depleted from total RNA using the rRNA depletion kit (NEB# E6310). After fragmentation of the ribosomal RNA–reduced RNA, complementary DNA (cDNA) was synthesized, ligated with the sequencing adapters, and amplified by PCR. The quality and yield were measured with the Fragment Analyzer (Agilent Technologies). The size of the products was consistent with the expected distribution (a broad peak between 300 and 500 bp). Clustering and DNA sequencing using the Illumina NextSeq 500 (Illumina) was performed according to manufacturer's protocols. A concentration of 1.6 pM of DNA was used. NextSeq control software 2.0.2 (https://support.illumina.com/downloads.html) was used. Image analysis, base calling, and quality check were performed with the Illumina data analysis pipeline Real-Time Analysis version 2.4.11 and Bcl2fastq version 2.17. Reads were aligned using the human assembly GRCh37.75. The reads were mapped to the reference sequence using a short read aligner based on Burrows—Wheeler Transform (Tophat version 2.0.14) with default settings.

RNA Sequencing Data Analysis

Sequencing data were normalized by fragments per kilobase of exon per million mapped fragments, and differential expression was assessed using DESeq2 (https://bioconductor.org/packages/release/bioc/html/DESeq2.html). Read counts were loaded into the DESeq2 package version 1.14.1 within the R platform version 3.3.0 to find differentially expressed (DE) genes between predefined sample groups. The output of this analysis was used to feed all 3 separate gene regulatory pathway enrichment tools.

Pathway analyses were performed using the Qiagen Ingenuity Pathway Analysis tool (Qiagen) and ErmineJ software (https://erminej.msl.ubc.ca/), using all DE genes with an adjusted p value $< .05$ to ensure the qualitative network analysis without a fold change cutoff. Weighted gene correlation networks were identified by weighted gene coexpression network analysis (WGCNA) (version 1.64) library in R (version 3.5.1). Data were converted into a matrix (DESeq2, version 1.20) where transcripts with a sum lower than 10 counts (all GM samples) were considered lowly expressed and removed

from the data frame. Variability among the samples was reduced by batch correction using sva (version 3.28.0) (22), where the number of the surrogate variables was predicted using the leek method (23). Genes with a mean count per million expression value in the lower-quartile range (25%) were removed to generate a signed network (beta value of 8) which was then used to perform hierarchical clustering on a topological overlap matrix. Only modules with 100 genes or more were merged with the mergeCloseModules (cutHeight = 0.25) function in the WGCNA package. The module eigengenes were recalculated to their corresponding modules and used to calculate the module-trait correlation between modules and age, sex, and cohort. The userListEnrichment function was applied, which provides cell type–specific gene expression profiles to compare the identified modules to previously observed networks. ClusterProfiler was used to annotate gene ontology terms for the identified WGCNA modules (24).

Immunohistochemistry

Formalin-fixed, paraffin-embedded 8-μm sections were cut, and antigen retrieval was accomplished in citrate buffer pH 6.0 (microwave, 10 minutes at 700 W). Endogenous peroxidase activity was blocked with 1% H_2O_2 for 20 minutes and nonspecific binding of secondary antibodies with 10% normal horse serum for 30 minutes. Sections were incubated with primary antibody (EDHu-1, 1:200; Novus Biologicals) overnight at 4 °C. The appropriate biotinylated (horse antimouse) secondary antibody was applied followed by conjugation with avidin-biotin horseradish peroxidase complex (Vector Elite ABC kit; Vector Laboratories). Visualization was established with DAB chromogen, and samples were counterstained with hematoxylin.

Images of stained tissue sections were taken using an Axioscope microscope Z1 (Zeiss) while using a Plan-Apochromat 20×/0.8 objective with a bright field camera (HV-F203SCL; Hitachi). Layer I to layer VI of the cortex and WM were manually outlined with Qupath 0.3.2 software (https://qupath.github.io/). The DAB background (color deconvolved) was measured for all sections. Subsequently, the DAB threshold for a positive signal was set at 4 times the average background. DAB particles with size between 10 and 100 mm^2, which exceeded the DAB threshold, were counted as $CD163^+$ cells.

Reverse Transcriptase–Quantitative PCR

cDNA synthesis was performed using the QuantiTect reverse transcription kit (Qiagen) according to manufacturer's instructions, with a minimal input of 200 ng total RNA. Quantitative PCR was performed using the 7300 Real Time PCR system (Applied Biosystems) using the equivalent cDNA amount of 1 to 2 ng total RNA used in cDNA synthesis. SYBRgreen mastermix (Applied Biosystems) and a 2 pmol/mL mix of forward and reverse primer sequences were used for 40 cycles of target gene amplification. For primer sequences, see Table S3. Expression of target genes was normalized to the average cycle threshold of *GAPDH* and *EF1A*. Cycle threshold values were assessed with Sequence Detection System software (http://appliedbiosystems.com/support/software/7900/updates.cfm; Applied Biosystems).

Synaptosome Isolation

Synaptosome fractions were isolated from frozen cortex tissue according to a public protocol from the Kelsey Martin lab that was adapted from Carlin *et al.* (25). In short, human cryostat sections (50 μm) were collected and stored in a disposable petri dish on dry ice. Sections were homogenized using a Dounce homogenizer in a sucrose-rich buffer with protease inhibition. Homogenates were spun down, pelleted, washed, and spun down at 1400*g* for 10 minutes to remove nuclei. Upon pelleting mitochondria and synaptosomes at 13,800*g* for 10 minutes, the pellet was resuspended in sucrose-rich buffer and layered on a gradient of 1.2M, 1.0M, and 0.85M sucrose buffer. After ultracentrifuge spinning at 82,500 for 2 hours, the top layer between 1.0M and 1.2M was aspirated off and processed further for protein detection.

Western Blotting

Isolated synaptosomes or brain tissue cryosections were lysed in cold radioimmunoprecipitation assay buffer containing 50mM Tris-HCl, pH 8.0, 150mM NaCl, 1% Nonidet-P40, 0.5% sodium deoxycholate, 0.1% sodium dodecyl sulfate, and protease inhibitors (complete EDTA-free; Sigma-Aldrich). Protein content was determined using the Pierce BCA Protein Assay kit (Thermo Fisher Scientific). For electrophoresis, proteins were separated by sodium dodecyl sulfate polyacrylamide gel electrophoresis and transferred to nitrocellulose Trans-Blot SD (BioRad). Blotted membranes were incubated in blocking buffer (5% bovine serum albumin in Tris-buffered saline with 0.05% Tween 20) for 1 hour followed by overnight incubation at 4 °C with primary antibodies directed against CD47 (B6H12.2; Novus Biologicals), CD200 (AF2724; R&D Systems), PSD95 (810401; BioLegend), or β-actin (AC-74; Sigma-Aldrich) in blocking buffer. After several washes with Tween 20, membranes were incubated with DyLight 649 (BioLegend) or IR800 (LI-COR)-conjugated secondary antibody for 1 hour at room temperature (1:2000 in blocking buffer). After washes in Tween 20, fluorescent signal was detected using the LI-COR Odyssey 9120 Imaging System (LI-COR).

Statistical Analysis

Statistical analysis of RT-qPCR, Western blot, and immunohistochemistry experiments was performed using GraphPad Prism version 9 software (https://www.graphpad.com/updates; GraphPad Software Inc.). Results are shown as mean with standard error of the mean. Statistical analysis was performed using either parametric or nonparametric testing based on the outcome of the Shapiro-Wilk normality test. The applied test for each calculated value is described in the figure legends. p Values $< .05$ were considered to indicate a significant difference.

RESULTS

Microglia Isolation Yields Pure Populations of Intact Microglia

In this study, we isolated intact microglia using a rapid isolation protocol from human occipital cortex GM and corpus callosum WM (Figure 1A). Flow cytometric phenotyping of intact microglia

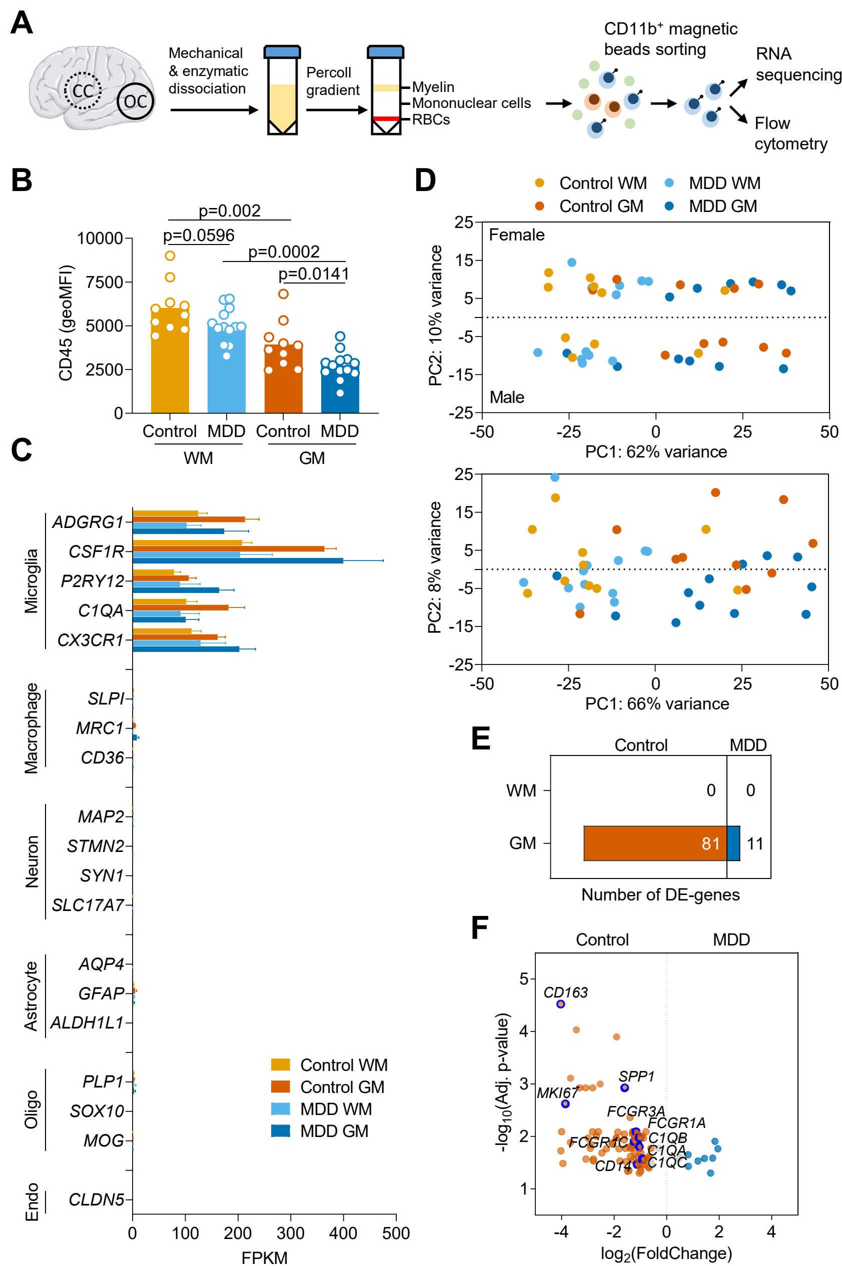

Figure 1. Differential gene expression in microglia isolated from MDD and control brain tissues determined by RNA sequencing. **(A)** Acute microglia isolation from WM (CC) and GM (OC) of 13 donors with MDD and 10 age-matched control donors by sorting CD11b^{+} magnetic beads. Flow cytometric analysis was performed, and RNA was isolated for RNA sequencing. **(B)** CD45 expression on GM and WM microglia detected by flow cytometry directly after isolation. Data passed the Kolmogorov-Smirnov normality test, and differences between MDD and control microglia were assessed using unpaired *t* tests. **(C)** Normalized expression of genes associated with microglia, neurons, astrocytes, oligodendrocytes, or endothelial cells in control WM or GM microglia. **(D)** PC analysis of gene expression demonstrates apparent differences between microglia from GM and WM and minor differences between microglia derived from female or male donors. **(E)** Number of DE genes for MDD vs. control microglia and for both WM and GM. **(F)** Volcano plot of DE genes between microglia obtained from donors with MDD or control donors. Threshold indicates DE genes with fold change $>$ 1.5, and purple circles indicate the notable downregulated genes of particular interest. Differential expression was determined using an adjusted p value (false discovery rate) $<$ .05. CC, corpus callosum; DE, differentially expressed; Endo, endothelial cells; FPKM, fragments per kilobase of exon per million mapped fragments; geoMFI, geometric mean fluorescent intensity; GM, gray matter; MDD, major depressive disorder; OC, occipital cortex; oligo, oligodendrocytes; PC, principal component; RBC, red blood cell; WM, white matter.

indicated no differences in CD11b expression, viability, and purity of microglia between donors with MDD (n = 13) and control (n = 10) donors (Figure S1). Membrane CD45 detection was lower in GM microglia isolated from donors with MDD (p = .0141), and for WM microglia, a trend toward decreased membrane CD45 in MDD was visible (p = .0596) (Figure 1B). RNA sequencing of isolated microglia from control GM or WM revealed enrichment of established microglial marker genes (*ADGRG1*, *CSF1R*, *P2RY12, C1QA*, *CX3CR1*) and no notable detection of macrophage (SLPI, MRC1, CD36), neuronal (*MAP2*, *STMN2*, *SYN1*, *SLC17A7*), astrocytic (*AQP4*, *GFAP*, *ALDH1L1*), oligodendrocytic (*PLP*, *SOX10*, *MOG*), or endothelial cell (*CLDN5*) marker genes (Figure 1C). As expected (20,26), hierarchical clustering of gene expression data showed that control GM and WM microglia were phenotypically distinct (Figure S2).

Microglial Samples Cluster Based on Region and Sex

Principal component analysis of microglial gene expression data of all samples revealed segregation of the samples in 4 groups, showing that the largest part of the variation was explained by regional differences between GM and WM

microglia (approximately 62%) (Figure 1D). Interestingly, the variance in principal component 2 was defined by sex (10%), with a similar effect in both GM and WM microglia. Further examination of DE genes between males and females only revealed Y chromosome genes and the X chromosome genes XIST and TSIX, for which expression from the inactive X chromosome accounts for the differential expression. Hence, no further analysis of these DE genes was performed. Cluster analysis of control samples only showed strong clustering of GM and WM samples; however, no complete segregation was seen. No apparent clustering of MDD or control samples was found in either GM or WM.

GM Microglia Show Differential Gene Expression in Donors With MDD

When comparing control GM and WM microglia using DESeq2 analysis, 2373 DE genes were found, as expected based on previous findings (26), of which 1691 were higher expressed in WM microglia and 682 were higher expressed in GM microglia. When comparing GM microglia isolated from MDD brains with control GM microglia, 92 DE genes passed multiple testing correction, of which 81 were lower expressed and 11 were higher expressed in MDD than in control microglia (Figure 1E, F). Notable downregulated genes encoded the scavenger receptor CD163, the proliferation marker Ki-67, the extracellular matrix protein osteopontin, the lipopolysaccharide coreceptor CD14, the high-affinity immunoglobulin gamma Fc receptor (CD64), and complement component C1q chains (see Table S4 for a complete list of all DE genes) (27,28). Regarding microglia isolated from WM, no DE genes passed multiple testing corrections between MDD and control donors.

To validate the top DE gene on protein level, CD163 immunohistochemistry staining was performed in occipital cortex GM of an independent, age-matched cohort of donors with MDD (n = 12) and control (n = 12) donors. CD163 was expressed by microglia and perivascular macrophages at lower levels in MDD (Figure 2A, B) (p = .028). Interestingly, CD163 staining intensity was the lowest in donors with a certain depressed state at the time of their death (Figure 2A, diamonds).

Effector Function Pathways Are Suppressed in GM MDD Microglia

Ingenuity Pathway Analysis was used to identify the genetic regulatory pathways associated with the DE genes in MDD compared with control GM microglia (Table 2, Figure 3). The largest part of implicated pathways showed lower activity in MDD GM microglia, with the top pathways being the complement system and Fc gamma receptor–mediated phagocytosis. Overlap in regulated genes between overrepresented pathways pointed to suppressed effector functions, specifically phagocytic activity of microglia, as indicated by nitric oxide and reactive oxygen species production by macrophages, pattern recognition of bacteria and viruses (indicating complement functioning), interleukin 12 signaling and production in macrophages, phagosome formation, and ceramide degradation (indicating cell membrane remodeling).

The gene score resampling approach gave nondirectional identified pathways that match overrepresented pathways listed in the Ingenuity Pathway Analysis. Gene ontology terms include IgG binding, macrophage activation, Fc gamma receptor signaling pathway, regulation of phagocytosis, plasma membrane invagination, phagocytosis, engulfment, and regulation of complement activation (Table S5). The comparison between WM microglia derived from either MDD or control donors that yielded no DE genes through DESeq2 analysis similarly only yielded one significant hit in the ErmineJ analysis (with false discovery rate $< .05$): extracellular matrix binding.

WGCNA identified clusters of coexpressed genes and allowed for multifactorial association analysis. When applied to the GM microglia samples with a minimum cluster size of 100 genes, WGCNA revealed 18 distinct modules (after merging related modules), which were further investigated in their association with 3 different group parameters: age, sex, and cohort (control or MDD) (Figure 4A). Module-trait relationship analysis showed 6 modules significantly related to cohort, 4 modules particularly related to age, and 2 modules especially related to sex. Of the cohort-related modules, 3 modules (M2, M4, and M9) were unique and not associated with age or sex, showing MDD-specific effects on overall gene expression patterns. M2, having the highest significant difference related to cohort, was of particular interest and included microglia function–related gene ontology terms, such as vesicle organization, cytosolic transport, and macroautophagy (Figure 4B).

Increased Suppression of Microglia in MDD GM

To explain a lower activation status of GM microglia in MDD, we examined the expression levels of CD47 and CD200, two well-known proteins involved in neuron-to-microglia signaling that silence microglial immune responses and prevent synaptic

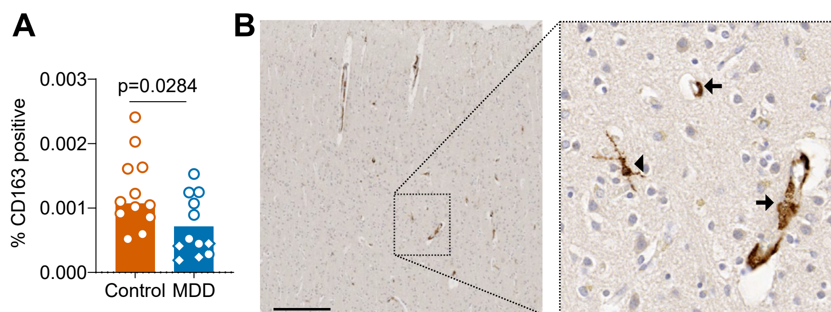

Figure 2. Immunohistochemical staining of CD163. An independent validation cohort of 12 donors with MDD and 12 age-matched control donors was selected, and formalin-fixed, paraffin-embedded tissue was extracted from the occipital cortex gray matter. **(A)** Immunoreactivity of CD163, presented as relative expression to total surface. Diamond-shaped symbols indicate donors with a definite depressed state when they died. **(B)** Representative images of CD163 staining of a control donor (40x magnification, scale bar = 250 μm), showing CD163^{+} microglia (arrowhead) and perivascular macrophages (arrow). Mann-Whitney U test: *$p < .05$. MDD, major depressive disorder.

Table 2. IPA Reveals Differential Expressed Signaling Pathways Between GM Microglia From Donors With MDD and Control Donors

Ingenuity Canonical Pathways	$-\log_{10}$ (Adjusted p Value)	Ratio	Genes
Complement System	3.43	0.0811	*C1QC, C1QA, C1QB*
Fcγ Receptor–Mediated Phagocytosis in Macrophages and Monocytes	3.38	0.0435	*NCK2, ARPC2, FCGR1A, FCGR3A/FCGR3B*
Production of Nitric Oxide and Reactive Oxygen Species in Macrophages	3.06	0.0258	*TLR2, MAP3K6, MAP3K8, SERPINA1, JAK3*
Role of Pattern Recognition Receptors in Recognition of Bacteria and Viruses	2.73	0.0292	*TLR2, C1QC, C1QA, C1QB*
Pyridoxal 5′-Phosphate Salvage Pathway	2.71	0.0462	*MAP3K6, PIM1, MAP3K8*
Salvage Pathways of Pyrimidine Ribonucleotides	2.22	0.0309	*MAP3K6, PIM1, MAP3K8*
iNOS Signaling	1.9	0.0444	*CD14, JAK3*
Phagosome Formation	1.85	0.0227	*TLR2, FCGR1A, FCGR3A/FCGR3B*
Iron Homeostasis Signaling Pathway	1.81	0.0219	*JAK3, CD163, SLC11A1*
CD27 Signaling in Lymphocytes	1.76	0.0377	*MAP3K6, MAP3K8*
IL-12 Signaling and Production in Macrophages	1.74	0.0205	*TLR2, MAP3K8, SERPINA1*
Actin Nucleation by ARP-WASP Complex	1.63	0.0323	*NCK2, ARPC2*
Ceramide Biosynthesis	1.58	0.143	*SPTLC2*
Ceramide Degradation	1.58	0.143	*ACER3*
TREM1 Signaling	1.48	0.0267	*TLR2, NLRC5*
Sphingosine and Sphingosine-1-Phosphate Metabolism	1.47	0.111	*ACER3*
Toll-like Receptor Signaling	1.47	0.0263	*TLR2, CD14*
VDR/RXR Activation	1.45	0.0256	*SPP1, CD14*
Calcium Transport I	1.43	0.1	*ATP2B4*
Dendritic Cell Maturation	1.42	0.0154	*TLR2, FCGR1A, FCGR3A/FCGR3B*

The ratio presented is defined as the number of the differentially expressed genes over the total number of genes involved in each of the pathways.

ARP-WASP, actin related protein—Wiskott–Aldrich syndrome protein; GM, gray matter; IL-12, interleukin 12; iNOS, inducible nitric oxide synthase; IPA, Ingenuity Pathway Analysis; MDD, major depressive disorder; RXR, retinoid X receptor; VDR, vitamin D receptor.

pruning (29–31). An independent cohort selection of MDD (n = 13) and age-matched control (n = 13) occipital cortex GM samples was used to investigate *CD47* and *CD200* expression by RT-qPCR (Figure 5A). While *CD47* showed a trend toward increased expression in MDD (p = .068), *CD200* was significantly higher expressed in MDD GM than in control GM (p = .0009) (Figure 5B). Because phagocytic pathways are implicated in microglia-mediated degradation of targeted synapses, we studied CD47 and CD200 expression in the synapse fraction of frozen human cortex. This synapse fraction is highly enriched for the excitatory postsynaptic marker PSD-95, detection of which is absent in the myelin fraction (Figure 5C). CD47 abundance was higher in MDD cortical synaptosomes than in those of controls (p = .0396), whereas CD200 was unchanged (Figure 5D, E).

DISCUSSION

Here, we showed that GM microglia, but not WM microglia, from donors with a clinical diagnosis of MDD, showed a distinct disease-associated microglia (DAM) transcriptomic profile that we have designated DepDAM. The majority of the DE genes (81 of 92) of GM microglia were downregulated, with numerous genes involved in immune responses (*MK167*, *SPP1*, *C1QA/B/C*) and phagocytic function (*FCGR1A/C*, *FCGR3A*, *CD14*, *CD163*). Consistent with individual genes, pathway analyses showed alterations in immune activation (complement system, inducible nitric oxide synthase signaling, interleukin 12 signaling) and phagocytic activity (regulation of phagocytosis, membrane invagination, phagocytosis, Fcγ receptor signaling in phagocytosis, interleukin 12, toll-like receptor, TREM1 signaling). Compared with control donors, an immune-suppressed state of MDD GM microglia was also apparent from a lower CD45 membrane expression assessed immediately after isolation.

Purified CD11b$^+$ cells expressed distinct microglial signature genes but lacked expression of genes defining macrophages, other glial lineages, or neurons (20). The homeostatic signature of GM microglia was unchanged in MDD, based on the unaltered expression of *ADGRG1*, *CSF1R*, *P2RY12*, and *CX3CR1*. Furthermore, there were no signs of immune

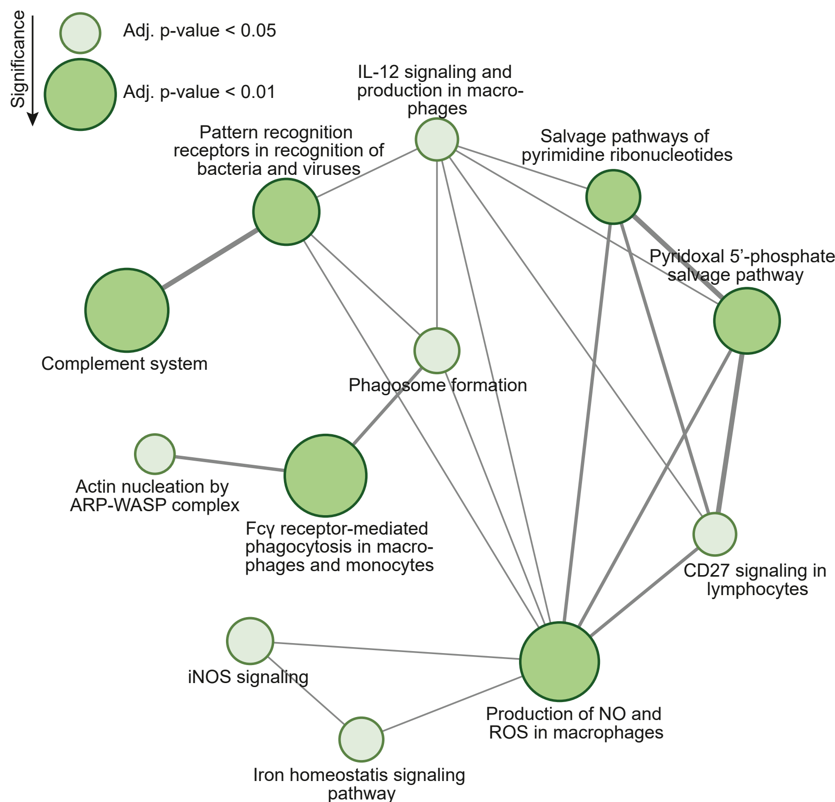

Figure 3. Map of enriched signaling pathways derived from the differentially expressed gene list between gray matter microglia from donors who had major depressive disorder and control donors, as determined by Ingenuity Pathway Analysis. Increasing node size indicates lower adjusted *p* value. Light green indicates an adjusted *p* value < .05; dark green indicates an adjusted *p* value < .01. Thicker lines between the nodes indicate a higher number of common differentially expressed genes between 2 pathways. Adj., adjusted; ARP-WASP, actin related protein—Wiskott–Aldrich syndrome protein; IL-12, interleukin 12; iNOS, inducible nitric oxide synthase; ROS, reactive oxygen species.

activation, such as increased expression of proinflammatory cytokines (*IL1*, *IL6*, *TNF*).

The DepDAM phenotype reported here is consistent with the results of several recent postmortem studies of donors with MDD (12,13,32–34) and may shed light on the underlying cause of failure of anti-inflammatory treatment trials in MDD (35,36). Snijders *et al.* (13) analyzed gene expression in microglia isolated from the medial frontal gyrus, superior temporal gyrus, thalamus, and subventricular zone in MDD using RT-qPCR and also identified a noninflammatory signature, which was based on reduced *CD163* and *CD14* expression but enhanced homeostatic gene (*TMEM119* and *CX3CR1*) activity. In a single-cell mass cytometry study, Böttcher *et al.* (12) found a noninflammatory microglia phenotype in MDD characterized by reduced human leucocyte antigen and CD68 expression and an increased homeostatic phenotype. Other studies have also found lower expression of microglial inflammatory genes in MDD dorsolateral prefrontal cortex tissue (33) and decreased expression of gene sets involved in endocytosis and antigen processing in the hippocampus and orbitofrontal cortex in MDD (32). As far as we know, our study is the first to have examined the transcriptome of acutely isolated postmortem microglia of MDD cortex, emphasizing the unbiased detection of pathways specifically implicated in DepDAM.

Taken together, these data are in contrast to earlier clinical findings using, for example, positron emission tomography imaging with radioligands for the TSPO receptor. This method has frequently been applied to indicate neuroinflammation in vivo. TSPO binding has been reported to be increased in several brain regions in MDD (19,37,38). However, the sensitivity and specificity of this method for detecting microglial activation in psychiatric disorders have been questioned (39,40). It should be emphasized that our autopsy cohort consists of MDD cases in a late phase, and it could be that inflammation and microglial activation do occur in earlier stages of the disease.

We only detected transcriptional differences in GM microglia and not in WM. This led us to the hypothesis that changes in microglia may be induced by neuronal interference. Indeed, here we showed increased expression of the neuronal “don’t eat me” signaling molecules CD200 and CD47 in tissue (CD200) and synaptosome fractions (CD47), potentially contributing to the dampened activation status of GM microglia in MDD (41,42). While neuroimmunomodulatory roles of CD47 and CD200 have been established, their influence on depressive symptoms has not been studied before. Given that the complement system and phagocytic functions are downregulated in cortical GM microglia, this may have implications for complement-mediated pruning of synapses. CD47 protects synapses from excess microglia-mediated pruning through signaling via the SIRP1α receptor on microglia during development and knockout of either CD47 or its receptor results in reduced synapse numbers (29). In addition, binding of CD200 to its receptor on myeloid cells (CD200R) is known to control microglial activity (30), and recently, it has been shown that CD200 deficiency leads to synaptic deficits and cognitive dysfunction (43,44). Microglia play an essential role in

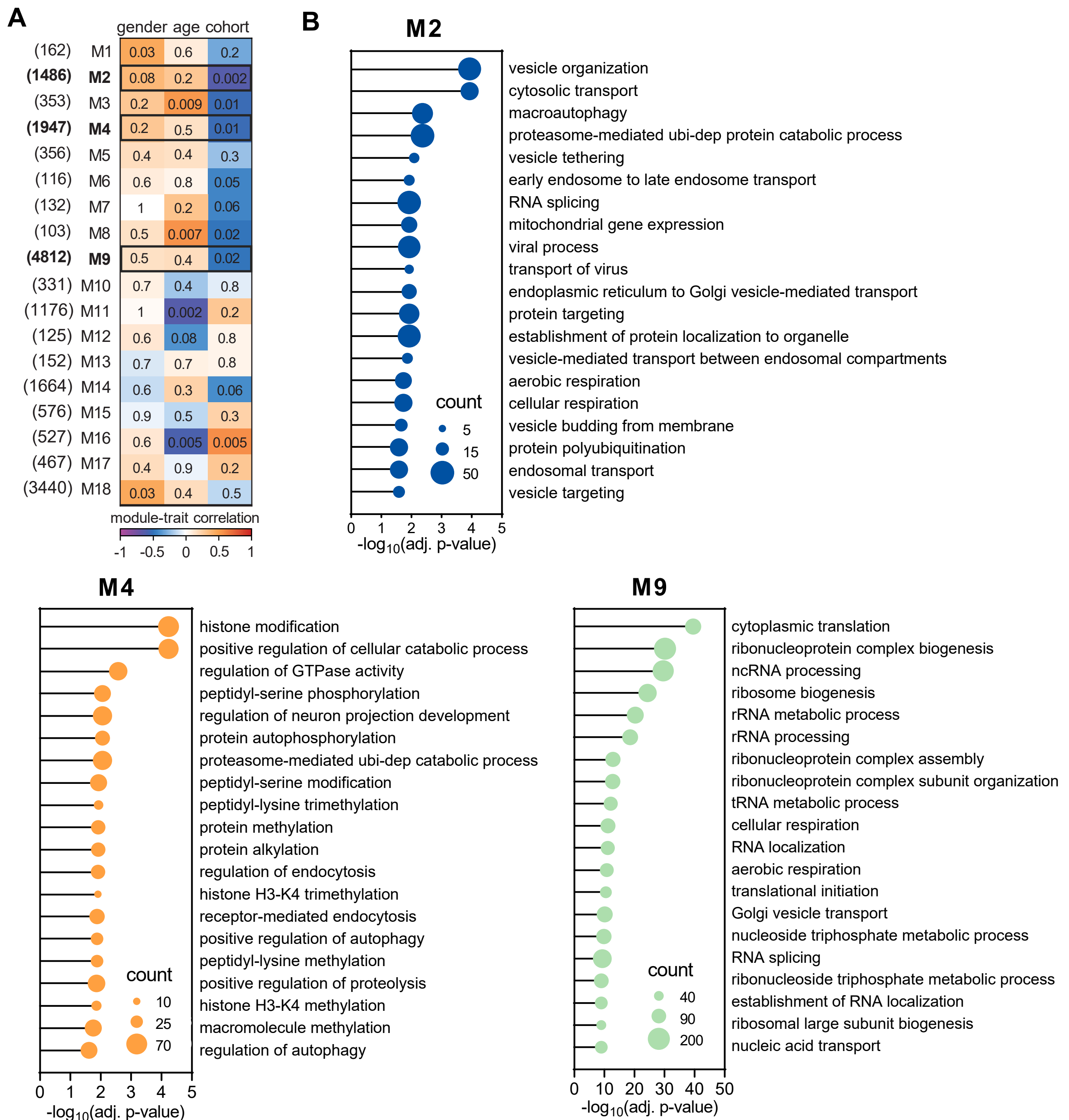

Figure 4. Coexpression networks for gray matter microglia from donors with major depressive disorder or control donors were determined by weighted gene correlation network analysis. **(A)** Eighteen modules identified are provided with their module-trait relationships and the number of genes that belong to each module displayed between brackets. Numbers in the heat map indicate the *p* value for the module-trait correlation. Minimum cluster size was set at 100 genes. **(B)** Gene ontology annotation of the genes in modules M2, M4, and M9, corresponding to overrepresented pathways in Ingenuity Pathway Analysis and ErmineJ analysis, visualized in a dot plot. The size of the dot represents the gene count. adj., adjusted; ncRNA, noncoding RNA; rRNA, ribosomal RNA; tRNA, transfer RNA; ubi-dep, ubiquitin-dependent.

synaptic circuit remodeling and phagocytosis of synaptic material, and defects may contribute to synaptic abnormalities seen in both neurodevelopmental and neurodegenerative diseases (45,46). Preclinical studies in depressed-like rodents showed microglial depletion with attenuated antidepressant and neurogenesis-enhancing treatment effects with imipramine or electroconvulsive stimulation (47). In addition, microglial stimulation in chronic, unpredictable

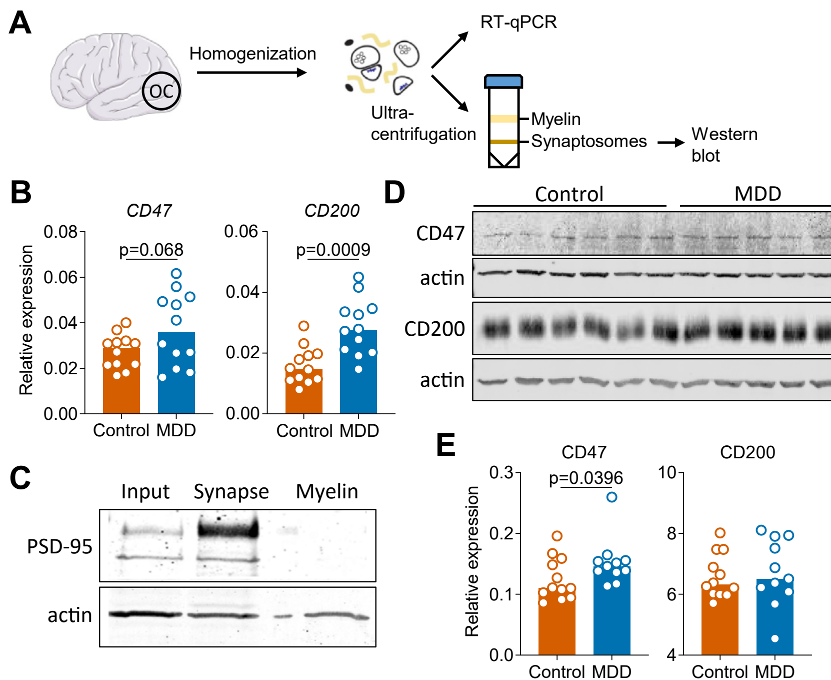

Figure 5. Increased suppression of microglia in MDD cortex. **(A)** An independent validation cohort of 13 donors with MDD and 13 age-matched control donors was selected. Frozen tissue was extracted from the OC for whole tissue RT-qPCR and Western blot analysis of synaptosomes. **(B)** Expression of CD200 and CD47 in MDD whole tissue determined by RT-qPCR. **(C)** Western blot analysis of PSD-95 expression in whole tissue homogenate (input), isolated synaptic fractions (synapse), and myelin fractions. **(D, E)** Western blot analysis of CD47 and CD200 expression in isolated synaptic fractions. MDD, major depressive disorder; OC, occipital cortex; RT-qPCR, reverse transcriptase–quantitative polymerase chain reaction.

stress-exposed mice with lipopolysaccharide or macrophage colony-stimulating factor reversed depressed-like behavior (48). One consistent finding in MDD pathology is the deficiency in functional synapses, which results in disruption of the neural circuits that underlie the regulation of mood (49–51). Chronic stress causes atrophy of neuronal processes and decreases in synaptic density, which are restored by newer rapid-acting antidepressants, such as esketamine (52,53).

Concerning limitations of the current study, almost all the MDD brain donors were treated with antidepressants, and we cannot rule out that these may have influenced the inflammatory status of microglia (54–57). Based on the lack of transcriptomic changes in WM microglia in MDD cases, it seems unlikely that the changes that we have described in GM microglia are a direct anti-inflammatory effect of medication. However, a secondary effect of medication through neuronal changes is possible. Control and MDD brain donors were matched for age, postmortem delay, and pH; however, the age did differ in the RNA sequencing group (75.0 vs. 63.7, p = .067), although the difference was not significant. Furthermore, information on the clinical state of depression at the time of death was unavailable for some donors. This may be important because it has been suggested that synaptic and neuroinflammatory changes in MDD may be state and severity dependent (51). However, more than half of our cohort died in a depressive state by euthanasia for refractory depression or suicide (7 of 13) (Table S1).

In summary, we found indications for an immune-suppressed GM microglial phenotype in the occipital cortex in MDD, possibly caused by neuronal regulation. An apathic microglial status with reduced phagocytosis and complement activation may have important consequences for synapse metabolism and connectivity relating to MDD. The DepDAM phenotype further adds to the continuum of microglia states that have been identified in the human brain (34).

ACKNOWLEDGMENTS AND DISCLOSURES

The Netherlands Brain Bank for Psychiatry (https://www.brainbank.nl/nbb-psy/) is funded by Grant No. 240–921200 from the Netherlands Organization for Scientific Research.

We thank the Psychiatric Donor Program of the Netherlands Brain Bank team for their excellent support and the donors for their valuable donation.

A previous version of this article was published as a preprint on medRxiv: https://doi.org/10.1101/2023.01.11.23284393.

After acceptance, the RNA sequencing dataset will be available online in the Gene Expression Omnibus database.

The authors report no biomedical financial interests or potential conflicts of interest.

ARTICLE INFORMATION

From the Neuroimmunology Research Group, Netherlands Institute for Neuroscience, Amsterdam, the Netherlands (KWFS, MRM, JvS, DDW, MRJM, C-CH, JH, IH); Psychiatric Program of the Netherlands Brain Bank, Netherlands Institute for Neuroscience, Amsterdam, the Netherlands (KWFS, MRM, JvS, AA, DDW, IH); Department of Psychiatry, Amsterdam University Medical Centers, Amsterdam Neuroscience, Amsterdam, the Netherlands (KWFS); Department of Biomedical Sciences of Cells and Systems, Section Molecular Neurobiology, University Medical Center Groningen, Groningen, the Netherlands (MLD, BJLE); Department of Experimental Immunology, Amsterdam Institute for Infection and Immunity, Amsterdam University Medical Centers, Amsterdam, the Netherlands (C-CH, JH); and Swammerdam Institute for Life Sciences, Center for Neuroscience, University of Amsterdam, Amsterdam, the Netherlands (IH).

KWFS and MRM contributed equally to this work as joint first authors. JH and IH contributed equally to this work as joint senior authors.

Address correspondence to Karel W.F. Scheepstra, Ph.D., at k.w.scheepstra@amsterdamumc.nl, or Inge Huitinga, Ph.D., at i.huitinga@nin.knaw.nl.

Received Feb 15, 2022; revised Feb 1, 2023; accepted Apr 17, 2023.
Supplementary material cited in this article is available online at https://doi.org/10.1016/j.biopsych.2023.04.020.

REFERENCES

1. GBD 2019 Diseases and Injuries Collaborators (2020): Global burden of 369 diseases and injuries in 204 countries and territories, 1990–2019: A systematic analysis for the Global Burden of Disease Study 2019. Lancet 396:1204–1222.
2. Rush AJ, Trivedi MH, Wisniewski SR, Nierenberg AA, Stewart JW, Warden D, *et al.* (2006): Acute and longer-term outcomes in depressed outpatients requiring one or several treatment steps: A STAR*D report. Am J Psychiatry 163:1905–1917.
3. Köhler CA, Freitas TH, Maes M, de Andrade NQ, Liu CS, Fernandes BS, *et al.* (2017): Peripheral cytokine and chemokine alterations in depression: A meta-analysis of 82 studies. Acta Psychiatr Scand 135:373–387.
4. Mariani N, Cattane N, Pariante C, Cattaneo A (2021): Gene expression studies in Depression development and treatment: An overview of the underlying molecular mechanisms and biological processes to identify biomarkers. Transl Psychiatry 11:354.
5. Eyre HA, Air T, Pradhan A, Johnston J, Lavretsky H, Stuart MJ, Baune BT (2016): A meta-analysis of chemokines in major depression. Prog Neuropsychopharmacol Biol Psychiatry 68:1–8.
6. Euesden J, Danese A, Lewis CM, Maughan B (2017): A bidirectional relationship between depression and the autoimmune disorders – New perspectives from the National Child Development Study. PLoS One 12:e0173015.
7. Andersson NW, Gustafsson LN, Okkels N, Taha F, Cole SW, Munk-Jørgensen P, Goodwin RD (2015): Depression and the risk of autoimmune disease: A nationally representative, prospective longitudinal study. Psychol Med 45:3559–3569.
8. Hoogland ICM, Houbolt C, van Westerloo DJ, van Gool WA, van de Beek D (2015): Systemic inflammation and microglial activation: Systematic review of animal experiments. J Neuroinflammation 12:114.
9. Hoogland ICM, Westhoff D, Engelen-Lee JY, Melief J, Valls Serón M, Houben-Weerts JHMP, *et al.* (2018): Microglial activation after systemic stimulation with lipopolysaccharide and Escherichia coli. Front Cell Neurosci 12:110.
10. Hendrickx DAE, van Scheppingen J, van der Poel M, Bossers K, Schuurman KG, van Eden CG, *et al.* (2017): Gene expression profiling of multiple sclerosis pathology identifies early patterns of demyelination surrounding chronic active lesions. Front Immunol 8:1810.
11. Ramaglia V, Dubey M, Malpede MA, Petersen N, de Vries SI, Ahmed SM, *et al.* (2021): Complement-associated loss of CA2 inhibitory synapses in the demyelinated hippocampus impairs memory. Acta Neuropathol 142:643–667.
12. Böttcher C, Fernández-Zapata C, Snijders GJL, Schlickeiser S, Sneeboer MAM, Kunkel D, *et al.* (2020): Single-cell mass cytometry of microglia in major depressive disorder reveals a non-inflammatory phenotype with increased homeostatic marker expression. Transl Psychiatry 10:310.
13. Snijders GJLJ, Sneeboer MAM, Fernández-Andreu A, Udine E, Psychiatric donor program of the Netherlands Brain Bank (NBB-Psy), Boks MP, *et al.* (2021): Distinct non-inflammatory signature of microglia in post-mortem brain tissue of patients with major depressive disorder. Mol Psychiatry 26:3336–3349.
14. Hammond BP, Manek R, Kerr BJ, Macauley MS, Plemel JR (2021): Regulation of microglia population dynamics throughout development, health, and disease. Glia 69:2771–2797.
15. Sneeboer MAM, Snijders GJLJ, Berdowski WM, Fernández-Andreu A, Psychiatric Donor Program of the Netherlands Brain Bank (NBB-Psy), van Mierlo HC, et al. (2019): Microglia in post-mortem brain tissue of patients with bipolar disorder are not immune activated. Transl Psychiatry 9:153.
16. Snijders GJLJ, van Zuiden W, Sneeboer MAM, Berdenis van Berlekom A, van der Geest AT, Schnieder T, *et al.* (2021): A loss of mature microglial markers without immune activation in schizophrenia. Glia 69:1251–1267.
17. Torres-Platas SG, Cruceanu C, Chen GG, Turecki G, Mechawar N (2014): Evidence for increased microglial priming and macrophage recruitment in the dorsal anterior cingulate white matter of depressed suicides. Brain Behav Immun 42:50–59.
18. Hannestad J, DellaGioia N, Gallezot JD, Lim K, Nabulsi N, Esterlis I, *et al.* (2013): The neuroinflammation marker translocator protein is not elevated in individuals with mild-to-moderate depression: A [^{11}C] PBR28 PET study. Brain Behav Immun 33:131–138.
19. Holmes SE, Hinz R, Conen S, Gregory CJ, Matthews JC, Anton-Rodriguez JM, *et al.* (2018): Elevated translocator protein in anterior cingulate in major depression and a role for inflammation in suicidal thinking: A positron emission tomography study. Biol Psychiatry 83:61–69.
20. Mizee MR, Miedema SSM, van der Poel M, Adelia SKG, Schuurman KG, van Strien ME, *et al.* (2017): Isolation of primary microglia from the human post-mortem brain: Effects of ante- and post-mortem variables. Acta Neuropathol Commun 5:16.
21. Melief J, Koning N, Schuurman KG, Van De Garde MDB, Smolders J, Hoek RM, *et al.* (2012): Phenotyping primary human microglia: Tight regulation of LPS responsiveness. Glia 60:1506–1517.
22. Leek JT, Johnson WE, Parker HS, Jaffe AE, Storey JD (2012): The SVA package for removing batch effects and other unwanted variation in high-throughput experiments. Bioinformatics 28:882–883.
23. Leek JT (2011): Asymptotic conditional singular value decomposition for high-dimensional genomic data. Biometrics 67:344–352.
24. Wu T, Hu E, Xu S, Chen M, Guo P, Dai Z, *et al.* (2021): clusterProfiler 4. 0: A universal enrichment tool for interpreting omics data. Innovation (Camb) 2:100141.
25. Carlin RK, Grab DJ, Cohen RS, Siekevitz P (1980): Isolation and characterization of postsynaptic densities from various brain regions: Enrichment of different types of postsynaptic densities. J Cell Biol 86:831–845.
26. van der Poel M, Ulas T, Mizee MR, Hsiao CC, Miedema SSM, Adelia, *et al.* (2019): Transcriptional profiling of human microglia reveals grey–white matter heterogeneity and multiple sclerosis-associated changes. Nat Commun 10:1139.
27. Masuda T, Sankowski R, Staszewski O, Böttcher C, Amann L, Sagar, *et al.* (2019): Spatial and temporal heterogeneity of mouse and human microglia at single-cell resolution. Nature 566:388–392.
28. Absinta M, Maric D, Gharagozloo M, Garton T, Smith MD, Jin J, *et al.* (2021): A lymphocyte–microglia–astrocyte axis in chronic active multiple sclerosis. Nature 597:709–714.
29. Lehrman EK, Wilton DK, Litvina EY, Welsh CA, Chang ST, Frouin A, *et al.* (2018): CD47 protects synapses from excess microglia-mediated pruning during development. Neuron 100:120–134.e6.
30. Barclay AN, Wright GJ, Brooke G, Brown MH (2002): CD200 and membrane protein interactions in the control of myeloid cells. Trends Immunol 23:285–290.
31. Elward K, Gasque P (2003): “Eat me” and “don’t eat me” signals govern the innate immune response and tissue repair in the CNS: Emphasis on the critical role of the complement system. Mol Immunol 40:85–94.
32. Darby MM, Yolken RH, Sabunciyan S (2016): Consistently altered expression of gene sets in postmortem brains of individuals with major psychiatric disorders. Transl Psychiatry 6:e890.
33. Pantazatos SP, Huang YY, Rosoklija GB, Dwork AJ, Arango V, Mann JJ (2017): Whole-transcriptome brain expression and exon-usage profiling in major depression and suicide: Evidence for altered glial, endothelial and ATPase activity. Mol Psychiatry 22:760–773.
34. Paolicelli RC, Sierra A, Stevens B, Tremblay ME, Aguzzi A, Ajami B, *et al.* (2022): Microglia states and nomenclature: A field at its crossroads. Neuron 110:3458–3483.
35. Miller AH, Pariante CM (2020): Trial failures of anti-inflammatory drugs in depression. Lancet Psychiatry 7:837.

36. Raison CL, Rutherford RE, Woolwine BJ, Shuo C, Schettler P, Drake DF, *et al.* (2013): A randomized controlled trial of the tumor necrosis factor antagonist infliximab for treatment-resistant depression: The role of baseline inflammatory biomarkers. JAMA Psychiatry 70:31–41.
37. Li H, Sagar AP, Kéri S (2018): Translocator protein (18 kDa TSPO) binding, a marker of microglia, is reduced in major depression during cognitive-behavioral therapy. Prog Neuropsychopharmacol Biol Psychiatry 83:1–7.
38. Setiawan E, Attwells S, Wilson AA, Mizrahi R, Rusjan PM, Miler L, *et al.* (2018): Association of translocator protein total distribution volume with duration of untreated major depressive disorder: A cross-sectional study. Lancet Psychiatry 5:339–347.
39. Sneeboer MAM, van der Doef T, Litjens M, Psy NBB, Melief J, Hol EM, *et al.* (2020): Microglial activation in schizophrenia: Is translocator 18-kDa protein (TSPO) the right marker? Schizophr Res 215:167–172.
40. Owen DR, Narayan N, Wells L, Healy L, Smyth E, Rabiner EA, *et al.* (2017): Pro-inflammatory activation of primary microglia and macrophages increases 18 kDa translocator protein expression in rodents but not humans. J Cereb Blood Flow Metab 37:2679–2690.
41. Biber K, Neumann H, Inoue K, Boddeke HWGM (2007): Neuronal "On" and "Off" signals control microglia. Trends Neurosci 30:596–602.
42. Koning N, Swaab DF, Hoek RM, Huitinga I (2009): Distribution of the immune inhibitory molecules CD200 and CD200R in the normal central nervous system and multiple sclerosis lesions suggests neuron-glia and glia-glia interactions. J Neuropathol Exp Neurol 68:159–167.
43. Loh KH, Stawski PS, Draycott AS, Udeshi ND, Lehrman EK, Wilton DK, *et al.* (2016): Proteomic analysis of unbounded cellular compartments: Synaptic clefts. Cell 166:1295–1307.e21.
44. Feng D, Huang A, Yan W, Chen D (2019): CD200 dysfunction in neuron contributes to synaptic deficits and cognitive impairment. Biochem Biophys Res Commun 516:1053–1059.
45. Paolicelli RC, Bolasco G, Pagani F, Maggi L, Scianni M, Panzanelli P, *et al.* (2011): Synaptic pruning by microglia is necessary for normal brain development. Science 333:1456–1458.
46. Schafer DP, Lehrman EK, Kautzman AG, Koyama R, Mardinly AR, Yamasaki R, *et al.* (2012): Microglia sculpt postnatal neural circuits in an activity and complement-dependent manner. Neuron 74:691–705.
47. Rimmerman N, Verdiger H, Goldenberg H, Naggan L, Robinson E, Kozela E, *et al.* (2022): Microglia and their LAG3 checkpoint underlie the antidepressant and neurogenesis-enhancing effects of electroconvulsive stimulation. Mol Psychiatry 27:1120–1135.
48. Kreisel T, Frank MG, Licht T, Reshef R, Ben-Menachem-Zidon O, Baratta MV, *et al.* (2014): Dynamic microglial alterations underlie stress-induced depressive-like behavior and suppressed neurogenesis. Mol Psychiatry 19:699–709.
49. Duman RS, Aghajanian GK, Sanacora G, Krystal JH (2016): Synaptic plasticity and depression: New insights from stress and rapid-acting antidepressants. Nat Med 22:238–249.
50. Kang HJ, Voleti B, Hajszan T, Rajkowska G, Stockmeier CA, Licznerski P, *et al.* (2012): Decreased expression of synapse-related genes and loss of synapses in major depressive disorder. Nat Med 18:1413–1417.
51. Holmes SE, Scheinost D, Finnema SJ, Naganawa M, Davis MT, DellaGioia N, *et al.* (2019): Lower synaptic density is associated with depression severity and network alterations. Nat Commun 10:1529.
52. Li N, Lee B, Liu RJ, Banasr M, Dwyer JM, Iwata M, *et al.* (2010): mTOR-dependent synapse formation underlies the rapid antidepressant effects of NMDA antagonists. Science 329:959–964.
53. Liu RJ, Lee FS, Li XY, Bambico F, Duman RS, Aghajanian GK (2012): Brain-derived neurotrophic factor Val66Met allele impairs basal and ketamine-stimulated synaptogenesis in prefrontal cortex. Biol Psychiatry 71:996–1005.
54. Basterzi AD, Aydemir C, Kisa C, Aksaray S, Tuzer V, Yazici K, Göka E (2005): IL-6 levels decrease with SSRI treatment in patients with major depression. Hum Psychopharmacol 20:473–476.
55. Ghareghani M, Zibara K, Sadeghi H, Dokoohaki S, Sadeghi H, Aryanpour R, Ghanbari A (2017): Fluvoxamine stimulates oligodendrogenesis of cultured neural stem cells and attenuates inflammation and demyelination in an animal model of multiple sclerosis. Sci Rep 7:4923.
56. Tynan RJ, Weidenhofer J, Hinwood M, Cairns MJ, Day TA, Walker FR (2012): A comparative examination of the anti-inflammatory effects of SSRI and SNRI antidepressants on LPS stimulated microglia. Brain Behav Immun 26:469–479.
57. Faissner S, Mishra M, Kaushik DK, Wang J, Fan Y, Silva C, *et al.* (2017): Systematic screening of generic drugs for progressive multiple sclerosis identifies clomipramine as a promising therapeutic. Nat Commun 8:1990.